Available online at www.sciencedirect.com
ScienceDirect
Biochemical and Biophysical Research Communications 355 (2007) 122–128
BBRC
www.elsevier.com/locate/ybbrc

Crystal structure and RNA-binding analysis of the archaeal transcription factor NusA

Rie Shibata [a], Yoshitaka Bessho [a,b], Akeo Shinkai [b], Madoka Nishimoto [a], Emiko Fusatomi [a], Takaho Terada [a,b], Mikako Shirouzu [a,b], Shigeyuki Yokoyama [a,b,c,*]

[a] *RIKEN Genomic Sciences Center, 1-7-22 Suehiro-cho, Tsurumi, Yokohama 230-0045, Japan*
[b] *RIKEN SPring-8 Center, Harima Institute, 1-1-1 Kouto, Sayo, Hyogo 679-5148, Japan*
[c] *Department of Biophysics and Biochemistry, Graduate School of Science, The University of Tokyo, 7-3-1 Hongo, Bunkyo-ku, Tokyo 113-0033, Japan*

Received 12 January 2007
Available online 31 January 2007

Abstract

The transcription factor NusA functions in transcriptional regulation involving termination in bacteria. A NusA homolog consisting of only the two KH domains is widely conserved in archaea, but its function remains unknown. We have found that *Aeropyrum pernix* NusA strongly binds to a certain CU-rich sequence near a termination signal. Our crystal structure of *A. pernix* NusA revealed that its spatial arrangement is quite similar to that of the KH domains of bacterial NusA. Thus, we consider archaeal NusA to have retained some functions of bacterial NusA, including the ssRNA-binding ability. Remarkable structural differences between archaeal and bacterial NusA exist at the interface with RNAP, in connection with the different NusA-binding sites around the termination signals. Transcriptional termination in archaea could differ from all of the known bacterial and eukaryal mechanisms, in terms of the combination of a bacterial factor and a eukaryal-type RNAP.

Keywords: Archaeal transcription; NusA; Termination signal; Crystal structure; KH domain

Transcription involves three stages: initiation, elongation, and termination, all of which are regulated by various factors and signal sequences. Bacteria and archaea possess one type of DNA-dependent RNA polymerase (RNAP), while eukarya have three types (RNAP I, II, III). The large subunits of all RNAPs, including the catalytic center, share sequence homology, suggesting that their fundamental reactions are similar [1]. However, differences in the minor components of the RNAP complexes between bacteria and eukarya suggest that the molecular mechanisms may vary in terms of the series of transcription events (Fig. 1A). In the termination stage, it is also known that both the termination signals and factors vastly differ between bacteria and eukarya.

Two types of termination (ρ-dependent and intrinsic [2,3]) systems function in bacterial transcription. The ρ-dependent mechanism requires a particular termination signal recognized by the ρ-protein. In intrinsic termination, a hairpin structure of nascent RNA, preceded by a stretch of U residues, is required as a transcription termination signal. Although the bacterial intrinsic termination partially functions with only the signal, it is further enhanced by the multifunctional transcription factor, NusA [4,5]. The eukaryal transcription termination systems differ entirely from the bacterial termination systems. For RNAP II, a C-terminal domain repeat extension (CTD) of the largest subunit, which regulates elongation and termination, serves as the assembly platform for termination factors [6,7]. The corresponding CTD region is missing in RNAP I and RNAP III. In

* Corresponding author. Address: RIKEN Genomic Sciences Center, Protein Research Group, 1-7-22 Suehiro-cho, Tsurumi, Yokohama 230-0045, Japan. Fax: +81 45 503 9195.
E-mail address: yokoyama@biochem.s.u-tokyo.ac.jp (S. Yokoyama).

0006-291X/$ - see front matter © 2007 Elsevier Inc. All rights reserved.
doi:10.1016/j.bbrc.2007.01.119

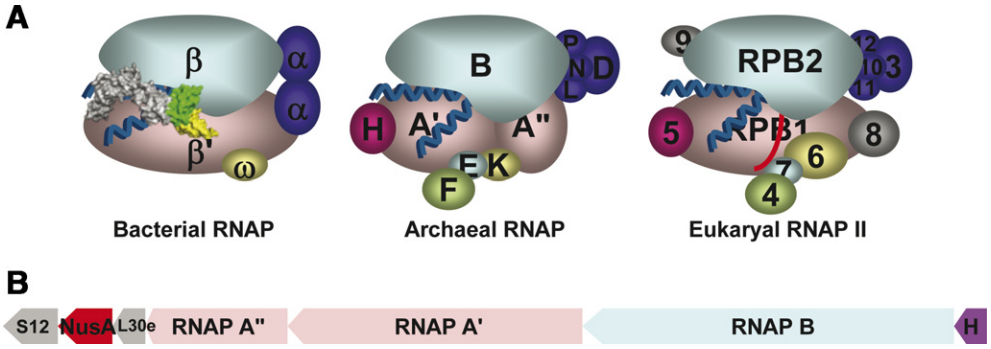

Fig. 1. (A) Schematic representation of RNAP components. The bacterial RNAP (left), archaeal RNAP (center), and eukaryal RNAP II (right) are shown. The docking model of bacterial NusA by Borukhov et al., is indicated on the bacterial RNAP (left) [23]. The two KH domains of bacterial NusA, colored green and yellow, are located near the RNA exit channel of bacterial RNAP. (B) The *A. pernix* NusA gene, located on the operon of the RNAP core components.

the latter complexes, other subunits (A12.6 for RNAP I and C11 for RNAP III), which share homology with the transcription cleavage factor TFIIS, and DNA- or RNA-binding proteins participate in transcription termination [8,9]. In all known eukaryal terminations, T-rich/U-rich DNA/RNA sequences are used for termination signals, although some differences exist in terms of the class of RNAP amongst various species.

In archaea, several sequences, including U-rich stretches and/or inverted repeats (hairpin), have been reported as termination signals [10,11]. However, the transcription termination mechanisms remain unclear. The archaeal RNAP more closely resembles the eukaryal RNAPs, rather than the bacterial RNAP, in terms of the components and the sequence homology between the large subunits [1]. The archaeal RNAP lacks the CTD of the largest subunit in RNAP II [12]. Almost all archaeal species have the cleavage factor TFS, which shares homology with the TFIIS involved with RNAP I and RNAP III, yet there is no evidence that it functions as a transcription termination factor in archaea [13].

A predicted orthologue of the bacterial transcription factor NusA is widely conserved in archaea [14]. The typical bacterial NusA contains an N-terminal domain (NTD), which interacts with RNAP, an S1 domain, and two RNA-binding K homology domains (KH) [15,16]. However, the archaeal NusA is unusually short, since it is composed of only the two tandem KH domains (Fig. S1A). Although the KH domains share low sequence homology with the corresponding domains of bacterial NusA (Fig. S1B), biological evidence suggests that the KH domains are important functional components for transcriptional events [17]. Thus, we predicted that it may participate in transcriptional events, considering that archaeal NusA is encoded in a cluster including the large RNAP subunits in almost all archaeal species (Fig. 1B) [14]. Therefore, we studied the archaeal NusA by confirming its RNA-binding ability and determining its crystal structure.

Materials and methods

NusA–RNA-binding analysis. We analyzed the interaction between *Aeropyrum pernix* NusA and various oligonucleotides with an SPR biosensor (Biacore 3000). Biotinylated RNA oligonucleotides (Dharmacon) were chemically synthesized with the sequences of 5′-GUGAGCGCCGCCUGAAAAGGCGGCGCUCGC-biotin-3′ (ds30S), 5′-GUGAGCGCCGCCU-biotin-3′ (ss13SL), 5′-AGGCGGCGCUCGC-biotin-3′ (ss13SR), 5′-CGCCUUCCCUCUU-biotin-3′ (ss13EX), 5′-GGAUGGAGGCGGCGCUCGCCUUCCCU-biotin-3′ (ds26H), 5′-GGAUGGAGGCGGC-biotin-3′ (ss13HL), poly-U13, poly-C13, poly-A13 and poly-G13. The biotinylated RNAs were immobilized onto commercially prepared SA sensor chips to yield an analyte R_{max} in the 650–800 RU range. All subsequent binding experiments were performed in 20 mM Hepes buffer (pH 7.0), containing 200 mM NaCl and 10 mM $MgCl_2$. RNA binding analyses involved from 25 to 7200 nM NusA, increased in at least five steps, at a flow rate of 20–25 μl/min for 2–2.5 min. The kinetic parameters and the dissociation constants (K_D) were determined from sensorgram data by using the BiaEvaluation 4.1 software package (Biacore AB).

Structure determination. The crystals of *A. pernix* wild-type NusA and selenomethionine-labeled NusA-I69M were obtained by the hanging-drop vapor diffusion method. The MAD data and the single wavelength data were collected at BL6A, Photon Factory and BL26B1, SPring8 (Japan), respectively. The atomic coordinates have been deposited in the Protein Data Bank, with the Accession Code 2CXC. The details of the crystallization and the structural calculations are described in the supplementary online material.

Results

The A. pernix NusA–RNA interaction

If the archaeal NusA participates in transcriptional termination in a similar manner as the bacterial NusA, then it should interact with the RNA in the vicinity of the termination sequences. The 23S rRNA termination signal was selected for the NusA-binding assay, since this region has been extensively studied in many species. The archaeal 16S and 23S rRNA genes are generally transcribed up to either pyrimidine (U- or CU-rich) stretches or an inverted repeat following the long, imperfect double helices with a bulge-helix-bulge motif for maturation of rRNAs (Fig. 2A) [18]. The termination site of the 23S rRNA from *Desulfurococcus mobilis*, which is in the same family as *A. pernix*, is mostly

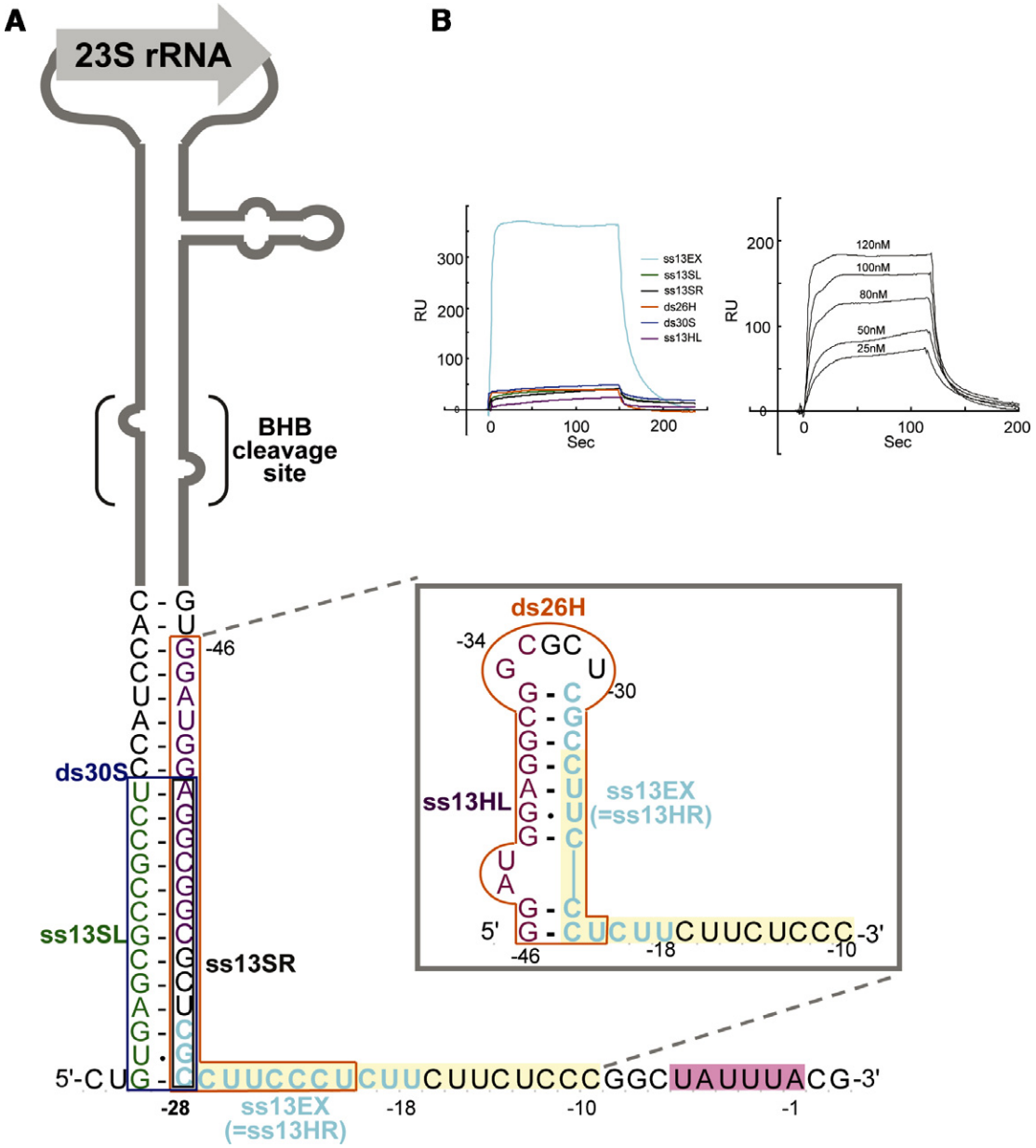

Fig. 2. (A) The secondary structure of the 23S rRNA flanking region in the rRNA operon from *A. pernix*. The long, imperfect double helices are preceded by predicted termination signals, stretches of CU-rich (shaded in yellow) and U-rich sequences (shaded in pink). The sequences of ss13SL (colored green), ss13SR (boxed in balck), and ds30S (boxed in blue) are from the terminus of the long stem. The sequence of ss13EX (colored cyan) is from the upstream region of the potential single-stranded termination signal. In the right panel, the alternative hairpin (boxed in orange) is named ds26H, and the upstream arm of the hairpin (colored purple) is called ss13HL. The downstream arm of the hairpin (ss13HR, cyan) is the same sequence as ss13EX. (B) Sensorgrams showing kinetic analyses of *A. pernix* NusA interacting with the various oligo RNAs shown in (A). In the left panel, each line represents the binding responses for NusA injections of 400 nM over the various nucleotide surfaces. The lines indicate RNAs in the same colors as in (A). In the right panel, several concentrations of NusA were used with ss13EX to calculate the dissociation constant (K_D).

after the long helices, but it can include stretches of U- and CU-rich sequences, as revealed by S1 mapping [19]. For *A. pernix* as well, the 23S rRNA gene flanks a long stem with a bulge–helix–bulge motif and stretches of U-rich (shaded pink in Fig. 2A) plus CU-rich (shaded yellow in Fig. 2A) sequences downstream [20]. These predicted termination signal sequences are preceded by an inverted repeat that forms an alternative stem loop (hairpin), like the bacterial intrinsic terminator (frame in Fig. 2A).

The Biacore 3000 binding assay results indicated that *A. pernix* NusA strongly interacts with the ss13EX RNA ($K_D = 5.6 \times 10^{-8}$ M), but only weakly or not at all with the other sequences (Fig. 2B and Table 1). This means that NusA specifically binds to a pyrimidine-rich sequence around the termination signal. Bacterial NusA reportedly interacts with the upstream arm of the hairpin RNA in intrinsic termination [4]. We also tested some RNAs (ds26H, ss13HL) derived from the alternative hairpin

Table 1
Binding affinities between NusA and RNAs, determined by Biacore analyses

RNA	K_D (M)
ss13EX	5.6×10^{-8}
ss13SL	1.5×10^{-5}
ss13SR	1.1×10^{-5}
ss13HL	3.3×10^{-6}
ds30S	2.5×10^{-6}
ds26H	1.3×10^{-6}
Poly-C13	1.4×10^{-8}
Poly-U13	8.0×10^{-7}
Poly-A13	5.9×10^{-7}
Poly-G13	NB

NB indicates no significant binding detected.

(frame in Fig. 2A). The results indicated that *A. pernix* NusA hardly binds to either the hairpin double stranded RNA (ds26H) or the upstream arm of the hairpin (ss13HL). To determine which kind of base in ss13EX contributes to NusA-binding, we assessed its binding ability to poly-U13, -C13, -A13, and -G13. The poly-C13 RNA strongly bound to NusA ($K_D = 1.4 \times 10^{-8}$ M), indicating that NusA binds to C preferentially.

Overall structure

The crystal structure of *A. pernix* NusA consists of two sterically adjacent KH domains, KH1 (residues 7–75) and KH2 (residues 76–144). Both KH domains comprise a three-stranded mixture of parallel and antiparallel β-sheets, which are packed against three α-helices (Fig. 3A). Their orders for KH1 and KH2 are α1–β1–β2–α2–α3–β3 and α4–β4–β5–α5–α6–β6, respectively. This is the typical type-II KH domain found most frequently in bacteria [21]. The topology of the *A. pernix* NusA is quite similar to the KH portions within the two bacterial crystal structures of NusA. When *A. pernix* NusA was superimposed with the KH domains of bacterial NusA proteins, the root mean squared deviations (RMSD) were 1.96 Å for the *Mycobacterium*

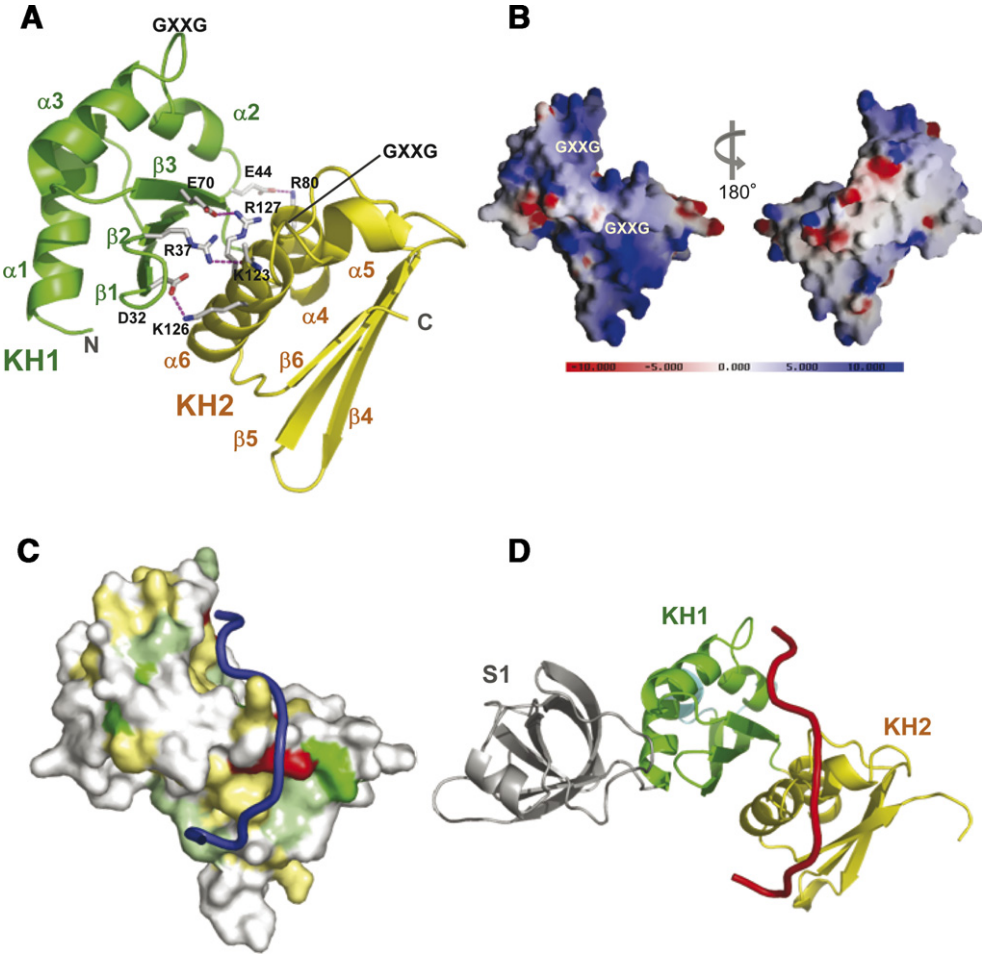

Fig. 3. The crystal structure of NusA from *A. pernix*. (A–D) Shown in the same viewpoint. (A) The individual domains (KH1: green, KH2: yellow) are shown by a ribbon model. Hydrogen bonded (dashed lines) residues between KH1 and KH2 are shown by stick models. (B) The electrostatic potential mapped onto the molecular surface of the *A. pernix* NusA. (C) The molecular surface of *A. pernix* NusA, color-coded according to amino acid sequence conservation, as in Fig. S1B. Red and yellow represent both bacterial and archaeal conservation, while green is only for archaea. The superimposed model of bacterial ssRNA on *A. pernix* NusA, shown as a blue tube [22]. (D) The crystal structure of the *M. tuberculosis* NusA and ssRNA complex [22]. The bacterial insertion region is colored light blue. The ssRNA is shown as a red-colored tube.

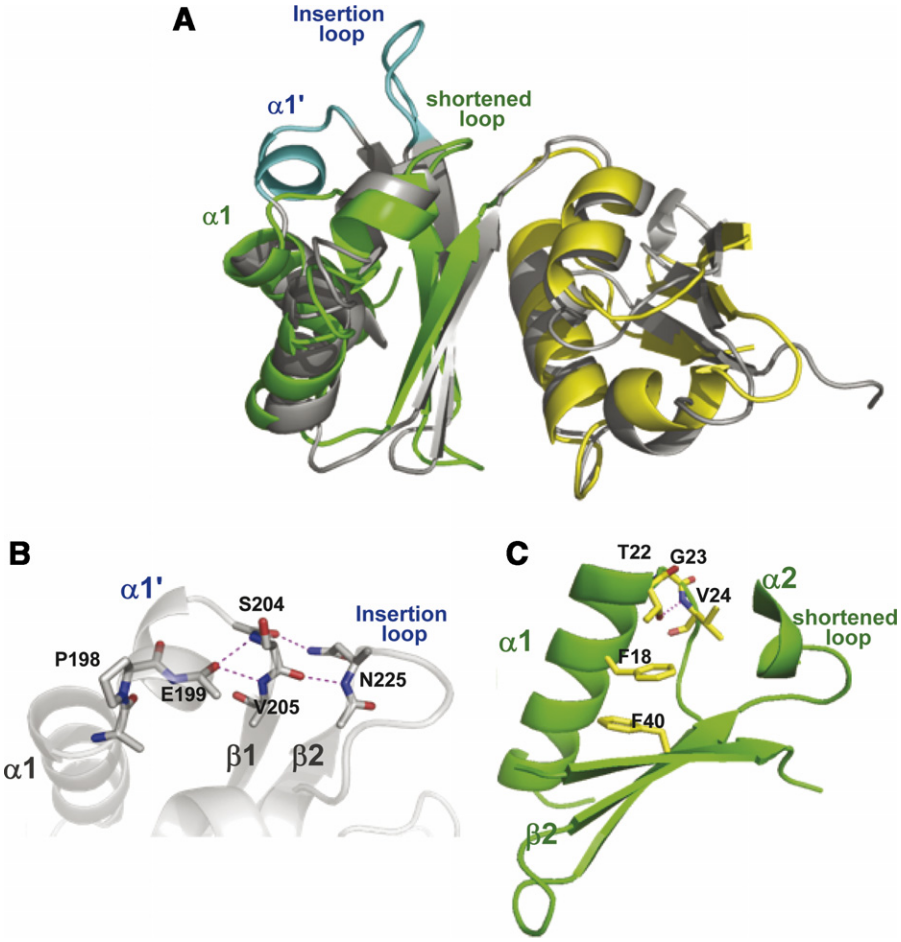

Fig. 4. (A) Superimposed model of the KH domains of *M. tuberculosis* (gray) [22] and *A. pernix* (green and yellow) NusA. The regions with the most differences between the bacterial and archaeal proteins are colored in light blue. (B,C) Detail of (A) in the most different region between the *M. tuberculosis* (B) and *A. pernix* (C) NusA molecules. The stick models indicate the residues that characteristically contribute to structural maintenance.

tuberculosis NusA and 1.93 Å for the *Thermotoga maritima* NusA [15,16] (Fig. 4A). Although the sequence identities between the *A. pernix* NusA and these bacterial NusA molecules are quite low (22%), the spatial arrangement of the two KH domains is significantly similar.

In the *A. pernix* NusA, KH1 interacts with KH2 in three areas, by hydrophobic and hydrogen-bonded interactions (Fig. 3A). In the first area, Glu44 (KH1) interacts with Arg80 (KH2) by a hydrogen-bond. In the second area, Asp32 (KH1) and Lys126 (KH2) make a salt bridge, supported by hydrophobic contacts with the surrounding residues (Tyr27, Leu41, Tyr74, Leu130, and Leu135). In the third area, Arg37 (KH1) and Lys123 (KH2), and Glu70 (KH1) and Arg127 (KH2) interact via hydrogen bonds. These residues forming the KH1–KH2 bridges are located in similar regions in bacterial NusA, in terms of both the sequence alignment and tertiary structure (boxed in light blue in Fig. S1B).

There is a concentration of positively charged residues on one side of the *A. pernix* NusA surface (Fig. 3B, left). The positively charged residues are especially concentrated in a loop between α2 and α3 (KH1), a central cleft defined by β3, α4, α5, and α6 (KH1, KH2), a loop between α5 and α6 (KH2), and a shelf formed by α6, β4, β5, and β6 (KH2). In the orientation shown in Fig. 3, the positively charged region forms a line from the top left (KH1) to the bottom right (KH2). Two helix–turn–helix (HTH) motifs (including the GXXG motif), conserved in the general KH domains located between α2 and α3 (KH1), and α5 and α6 (KH2), lie on this positively charged line. The angles between the respective helices of the HTH motifs are also the same as those in the bacterial NusA (Fig. 3D). In contrast, the inverse surface (Fig. 3B, right) consists of many hydrophobic residues, with some negatively charged loops.

Detailed structure

The arrangement of the *A. pernix* helices and sheets corresponds to the representative type II KH domain (Fig. 4A). In the *M. tuberculosis* NusA structure, the bacterial conserved Pro198 disrupts the first helix, resulting in two new helices (α1 and α1′) oriented at 90° relative to each other (Fig. 4B). As compared to the bacterial NusA, the archaeal-conserved Phe18 of *A. pernix*, which corresponds to the bacterial Pro198, stacks with the archaeal-

conserved Phe40 (or Tyr40) of β2 (Fig. 4C). Therefore, the α1 helix in the archaeal NusA structure is stabilized.

The extra α1′ helix in bacteria is stabilized by hydrogen bonds in the long loop between β2 and α2 in the KH1 domain (Fig. 4B). The corresponding loop between β2 and α2 of *A. pernix* is much shorter than that in the bacterial NusA, and is not needed to stabilize the α1′ helix via hydrogen-bonds (Fig. 4C). Instead, the *A. pernix* α1 helix ends at the conserved Thr22, with its side chain forming a hydrogen bond with the main chain of Val24 (Fig. 4C). Since both of these features are missing in the *A. pernix* structure, the resultant effect is a reduction in the overall size of the molecule by 7 Å in the KH1 region.

In the *A. pernix* KH2 domain, three β-strands (β4, β5, and β6) were one to three residues longer than those in bacterial NusA. This causes the KH2 domain about 6 Å larger than that in bacterial NusA, as shown in the lower part of Fig. 3A. These residues contribute to the positive charge mentioned above.

Discussion

The structure of *A. pernix* NusA is quite similar to that composed of the KH domains of bacterial NusA, in terms of the secondary structure and the domain arrangement [15,16]. A plot of the archaeal (and bacterial) conserved residues on the surface of *A. pernix* NusA revealed that most were localized on the positively charged surface, including the GXXG motif (Fig. 3B, left and C). In the bacterial NusA, these positively charged residues reportedly associate with single stranded RNA on a large surface formed by both bacterial KH domains (Fig. 3D) [22]. The more basic surface of archaeal NusA might facilitate the interaction with its RNA targets. In the docking model of bacterial NusA and RNAP by Borukhov et al., the two KH domains are located near the RNA exit channel formed by the β flap and the clamp domain of RNAP [23]. This is consistent with other cross-linking, biochemical, and genetic data [24]. The β flap ('wall' in RNAP II) and the clamp domain of bacterial RNAP are also structurally conserved with the those of the eukaryotic RNAP II [25,26]. In spite of the lack of structural reports, the significant sequence homology suggests that the structure of archaeal RNAP should be basically similar to those of the bacterial and eukaryal RNAPs. Therefore, in consideration of the structural similarity of the KH domains, the archaeal NusA might be able to interact with the archaeal RNAP, even though the archaeal RNAP more closely resembles the eukaryal RNAP than the bacterial RNAP (Fig. 1A). The most obviously different region of KH1 between the bacterial and archaeal NusA proteins (top left in Fig. 4A) exists on the interface side for RNAP in the docking model (Fig. 1A, left), suggesting a relationship with a different kind of RNAP.

In the *A. pernix* rRNA operon, a pyrimidine-rich stretch (shaded yellow) and/or a U-rich stretch (shaded pink), were considered as termination signal candidates (Fig. 2). The results of our binding assay indicated that *A. pernix* NusA binds ss13EX more strongly than the other sequences. The structures of the bacterial and eukaryal RNAPs and their protection experiments revealed that the nascent RNA transcript forms a hybrid with the DNA (at positions +1 to −8), and the transcript is enclosed to around −14 or −17 [27,28]. We propose that the *A. pernix* 23S rRNA terminates, depending on the archaeal NusA and pyrimidine-rich signal preceding the U-rich stretch (shaded pink), because of the proper distance (18 nt) between ss13EX and the U-rich stretch. Archaeal NusA could have retained some functions of bacterial NusA, including the ssRNA-binding ability, which regulates various transcriptional events [23].

In bacterial intrinsic termination, the KH-domains of the NusA protein bind to the single stranded upstream arm of the hairpin RNA [4,5]. However, since the archaeal NusA of *A. pernix* dose not interact with the ss13HL RNA of the potential hairpin RNA, there are still some differences from the bacterial intrinsic termination. In the eukaryotic RNAP II, the termination signal sequences recognized by the termination factors are situated far upstream of the termination site. Since the archaeal RNAP lacks the corresponding region of the CTD, the termination of *A. pernix* rRNAs must differ from that by the eukaryal RNAP II [12]. In the eukaryotic RNAP I, a stretch of Ts in the DNA is recognized by a DNA-binding termination factor, but RNA-binding proteins as termination factors have not been reported [29]. In the eukaryotic RNAP III, termination depends on U stretches and a component of RNAP III supported by the La protein, which lacks an archaeal homolog [30]. In contrast, a NusA homolog has not been found in eukarya, and therefore, the transcription termination in archaea differs from that in eukarya, in terms of the use of a bacterial-type transcription factor with a eukaryal type of RNAP.

Acknowledgments

We thank Dr. Kazutaka Murayama, Dr. Peter H. Rehse, Dr. Tatsuya Kaminishi and Ms. Miyuki Kato-Murayama for discussions. This work was supported by the RIKEN Structural Genomics/Proteomics Initiative (RSGI), the National Project on Protein Structural and Functional Analyses, the Ministry of Education, Culture, Sports, Science and Technology of Japan.

Appendix A. Supplementary data

Supplementary data associated with this article can be found, in the online version, at doi:10.1016/j.bbrc.2007.01.119.

References

[1] P. Cramer, Multisubunit RNA polymerases, Curr. Opin. Struct. Biol. 12 (2002) 89–97.

[2] J.P. Richardson, Rho-dependent termination and ATPases in transcript termination, Biochim. Biophys. Acta 1577 (2002) 251–260.
[3] Y. d'Aubenton Carafa, E. Brody, C. Thermes, Prediction of rho-independent *Escherichia coli* transcription terminators. A statistical analysis of their RNA stem-loop structures, J. Mol. Biol. 216 (1990) 835–858.
[4] I. Gusarov, E. Nudler, Control of intrinsic transcription termination by N and NusA: the basic mechanisms, Cell 107 (2001) 437–449.
[5] I. Toulokhonov, I. Artsimovitch, R. Landick, Allosteric control of RNA polymerase by a site that contacts nascent RNA hairpins, Science 292 (2001) 730–733.
[6] M. Kim, N.J. Krogan, L. Vasiljeva, O.J. Rando, E. Nedea, J.F. Greenblatt, S. Buratowski, The yeast Rat1 exonuclease promotes transcription termination by RNA polymerase II, Nature 432 (2004) 517–522.
[7] S. West, N. Gromak, N.J. Proudfoot, Human 5′→3′ exonuclease Xrn2 promotes transcription termination at co-transcriptional cleavage sites, Nature 432 (2004) 522–525.
[8] E.M. Prescott, Y.N. Osheim, H.S. Jones, C.M. Alen, J.G. Roan, R.H. Reeder, A.L. Beyer, N.J. Proudfoot, Transcriptional termination by RNA polymerase I requires the small subunit Rpa12p, Proc. Natl. Acad. Sci. USA 101 (2004) 6068–6073.
[9] S. Chedin, M. Riva, P. Schultz, A. Sentenac, C. Carles, The RNA cleavage activity of RNA polymerase III is mediated by an essential TFIIS-like subunit and is important for transcription termination, Genes Dev. 12 (1998) 3857–3871.
[10] J.W. Brown, C.J. Daniels, J.N. Reeve, Gene structure, organization, and expression in archaebacteria, Crit. Rev. Microbiol. 16 (1989) 287–338.
[11] T.J. Santangelo, J.N. Reeve, Archaeal RNA polymerase is sensitive to intrinsic termination directed by transcribed and remote sequences, J. Mol. Biol. 355 (2006) 196–210.
[12] E.P. Geiduschek, M. Ouhammouch, Archaeal transcription and its regulators, Mol. Microbiol. 56 (2005) 1397–1407.
[13] U. Lange, W. Hausner, Transcriptional fidelity and proofreading in Archaea and implications for the mechanism of TFS-induced RNA cleavage, Mol. Microbiol. 52 (2004) 1133–1143.
[14] N.C. Kyrpides, C.A. Ouzounis, Transcription in archaea, Proc. Natl. Acad. Sci. USA 96 (1999) 8545–8550.
[15] M. Worbs, G.P. Bourenkov, H.D. Bartunik, R. Huber, M.C. Wahl, An extended RNA binding surface through arrayed S1 and KH domains in transcription factor NusA, Mol. Cell 7 (2001) 1177–1189.
[16] B. Gopal, L.F. Haire, S.J. Gamblin, E.J. Dodson, A.N. Lane, K.G. Papavinasasundaram, M.J. Colston, G. Dodson, Crystal structure of the transcription elongation/anti-termination factor NusA from *Mycobacterium tuberculosis* at 1.7 Å resolution, J. Mol. Biol. 314 (2001) 1087–1095.
[17] Y. Zhou, T.F. Mah, J. Greenblatt, D.I. Friedman, Evidence that the KH RNA-binding domains influence the action of the *E. coli* NusA protein, J. Mol. Biol. 318 (2002) 1175–1188.
[18] H. Leffers, J. Kjems, L. Ostergaard, N. Larsen, R.A. Garrett, Evolutionary relationships amongst archaebacteria. A comparative study of 23S ribosomal RNAs of a sulphur-dependent extreme thermophile, an extreme halophile and a thermophilic methanogen, J. Mol. Biol. 195 (1987) 43–61.
[19] J. Kjems, R.A. Garrett, Novel expression of the ribosomal-RNA genes in the extreme thermophile and archaebacterium *Desulfurococcus mobilis*, EMBO J. 6 (1987) 3521–3530.
[20] N. Nomura, Y. Morinaga, N. Shirai, Y. Sako, I-ApeKI [corrected]: a novel intron-encoded LAGLIDADG homing endonuclease from the archaeon, *Aeropyrum pernix* K1, Nucleic Acids Res. 33 (2005) e116.
[21] N.V. Grishin, KH domain: one motif, two folds, Nucleic Acids Res. 29 (2001) 638–643.
[22] B. Beuth, S. Pennell, K.B. Arnvig, S.R. Martin, I.A. Taylor, Structure of a *Mycobacterium tuberculosis* NusA–RNA complex, EMBO J. 24 (2005) 3576–3587.
[23] S. Borukhov, J. Lee, O. Laptenko, Bacterial transcription elongation factors: new insights into molecular mechanism of action, Mol. Microbiol. 55 (2005) 1315–1324.
[24] S.L. Traviglia, S.A. Datwyler, D. Yan, A. Ishihama, C.F. Meares, Targeted protein footprinting: where different transcription factors bind to RNA polymerase, Biochemistry 38 (1999) 15774–15778.
[25] D.G. Vassylyev, S. Sekine, O. Laptenko, J. Lee, M.N. Vassylyeva, S. Borukhov, S. Yokoyama, Crystal structure of a bacterial RNA polymerase holoenzyme at 2.6 Å resolution, Nature 417 (2002) 712.
[26] P. Cramer, D.A. Bushnell, R.D. Kornberg, Structural basis of transcription: RNA polymerase II at 2.8 angstrom resolution, Science 292 (2001) 1863–1876.
[27] N. Korzheva, A. Mustaev, M. Kozlov, A. Malhotra, V. Nikiforov, A. Goldfarb, S.A. Darst, A structural model of transcription elongation, Science 289 (2000) 619–625.
[28] A.L. Gnatt, P. Cramer, J. Fu, D.A. Bushnell, R.D. Kornberg, Structural basis of transcription: an RNA polymerase II elongation complex at 3.3 Å resolution, Science 292 (2001) 1876–1882.
[29] R.H. Reeder, W.H. Lang, Terminating transcription in eukaryotes: lessons learned from RNA polymerase I, Trends Biochem. Sci. 22 (1997) 473–477.
[30] Y. Huang, R.V. Intine, A. Mozlin, S. Hasson, R.J. Maraia, Mutations in the RNA polymerase III subunit Rpc11p that decrease RNA 3′ cleavage activity increase 3′-terminal oligo(U) length and La-dependent tRNA processing, Mol. Cell. Biol. 25 (2005) 621–636.